Proceedings of the Institute of Acoustics

COUPLED OCEAN-ACOUSTIC MODELLING STUDIES OF OCEAN FRONTS AND EDDIES

A D Heathershaw and M R Gething

Admiralty Research Establishment, Southwell, Portland, Dorset, DT5 2JS, UK

1. INTRODUCTION

Low frequency sonar permits detection over ranges comparable with the mesoscale variability of the ocean. In order to be able to make full use of this capability, accurate acoustic predictions require realistic simulations of the in-water environment. Supercomputers and remote sensing of the oceans by satellite now bring the goal of global eddy resolving ocean prediction models within our reach [1,2]. In both the USA [3] and UK [4], navy operational ocean forecast systems are being developed that will predict the ocean environment for input into range-dependent acoustic models. Such systems will entail the use of 1-D and 3-D numerical models. However, it is by no means clear that such models will adequately resolve upper ocean processes and mesoscale variability for acoustic purposes. Not only do we need to be able to understand the sensitivity of the acoustic predictions to changes in the model generated environments but also their sensitivity to the ocean model parameters. The latter may include horizontal and vertical resolution but more importantly will include parameters that reflect any uncertainty in the ocean model physics. For example, eddy viscosity and diffusion coefficients are used to describe processes that occur on scales that are too small to be resolved by numerical model grids. The values of these coefficients are more often chosen with computational requirements in mind than for their physical representativeness. How then do we study this problem? One solution is to run ocean and acoustic models together, the so-called coupled ocean-acoustic modelling approach.

2. COUPLED OCEAN-ACOUSTIC MODEL DEVELOPMENT

Research during the 1970s and early 1980s showed that it was possible to study the effects of ocean fronts and eddies on sound propagation, using generalised models of these features. For example, Henrick et al [5,6] developed an analytical model of mesoscale ocean eddies which made it possible to relate acoustic properties to eddy size and strength, including currents. This model was subsequently used by Baer [7], in conjunction with a 3-D acoustic model, to study horizontal and vertical refraction effects due to eddies. Similarly, Rousseau et al [8] used an idealised model of an ocean front to study its effect on short range acoustic transmissions.

A limitation of these studies has been their use of analytical models to describe isolated features and their inability to evolve frontal and eddy-like features realistically in space and time. This has had to await the development of sophisticated numerical model codes and powerful computers to achieve the desired resolution. However, 1-D numerical models of the upper ocean have been used in coupled ocean-acoustic model investigations of surface duct propagation [9,10]. Such models, which are less demanding of computer resources than 3-D models, have formed the basis of most early naval ocean prediction systems, for example the US Navy's TOPS [3,11] and the Royal Navy's NEAT MLM system [4]. Coupled ocean-acoustic model studies of the upper ocean have provided valuable insights into the way in which sound propagates in the surface mixed layer. For example, Porter et al [12] used a number of 1-D mixed layer models to illustrate how differences in

the predicted, near-surface, thermal structures can have a significant effect on sound propagation characteristics.

Such studies have employed 1-D ocean model schemes and range-independent acoustic models. However, to study the sensitivity of the acoustics to changes in the mesoscale environment requires a different approach. Such an approach is provided by 3-D numerical ocean models in which the time varying fields of temperature and salinity can be properly described. Additionally, it is necessary to employ 2-D or 3-D acoustic models. Research along these lines has only recently begun. For example Botseas and Seigmann [13] and Melberg et al [14] describe the coupling together of a range-dependent acoustic model (the Implicit Finite Difference (IFD) model [15]) with the Harvard Open Ocean Model [16]. Using a combination of observed oceanographic conditions and feature models, the Harvard model was used to forecast eddy and frontal structures in the Gulf Stream which could then be input to acoustic models. In particular, the coupled models were used to examine the temporal variability in acoustic propagation through a Gulf Stream meander and eddies. While Melberg et al [14] have demonstrated that coupled ocean-acoustic models may be used to study the temporal variability of acoustic propagation through modelled frontal and eddy features, their study did not specifically address the sensitivity of acoustic predictions to ocean model parameters.

In this paper we describe the development of a coupled ocean-acoustic modelling approach, using both 1-D and 3-D numerical ocean models, to address just this problem. Consideration of geometrical spreading loss and frequency-dependent volume attenuation in a surface duct leads to simple arguments concerning acoustic sensitivity, in particular to changes in propagation loss as a result of changes in duct depth and near-surface temperature gradients. The results from simulations with an atmospherically forced 1-D mixed layer model are then used to illustrate these ideas, in particular the requirements for vertical resolution in ocean models.

Range-dependent acoustic sensitivity calculations have also been performed using a 3-D numerical ocean model to simulate eddies at an ocean front and to provide synoptic estimates of the sound speed field throughout the frontal region for input to acoustic models. These data are used to test the sensitivity of the acoustic predictions to changes in ocean model parameters, in particular the parameterisation of processes that are too small to be resolved by the numerical model grids, but which may still be important for the acoustics.This approach has direct relevance to the development of naval ocean forecast models where the overall setting of ocean model parameters may be determined by computational requirements rather than a desire to achieve realistic simulations for acoustic purposes.

3. OCEAN MODELS

In this section we briefly illustrate the types of model that are used in ocean-acoustic simulations. Many ocean models exist which provide different formulations of the physics in both one dimension and in three dimensions. Our object here is to illustrate the essential physics and to identify the ocean model parameters that are likely to be of significance in performing ocean-acoustic simulations.

In general, three main types of model have been used to study the deep ocean over periods of days to years. The first of these to be developed was the primitive equation model of Bryan and Cox

[17-20]. This uses a simple advection equation for temperature and salinity, and for the velocities it uses a momentum equation in the horizontal and a continuity equation in the vertical. Computational efficiency is achieved by imposing a 'rigid lid' restriction on the surface of the ocean which prevents the generation of surface gravity waves. The fastest waves in the model are then the internal gravity waves, and their slow speed allows the use of a longer time step.

In a second class of model, the quasi-geostrophic model [21-23], an even longer time step is possible by filtering out the internal waves. However, to do this a number of approximations are necessary. The first of these is an assumption that the model is in geostrophic balance (see later). Such an approximation is expected to break down near fronts and in regions where the eddy sizes are small. Such models also cannot be used near the equator. The second approximation made is that there are no changes in temperature and salinity due to surface cooling, diffusion or large scale vertical advection. Such a model would not be suitable in the North Atlantic where there are large horizontal changes in density, for example where fronts outcrop at the surface and where winter cooling is important.

A third class of model, the isopycnal coordinate model [24], is currently under development. These models are similar to the Bryan and Cox primitive equation model described previously, except that the equations are solved on density surfaces. These models have an advantage in that away from ocean boundaries they conserve vorticity better than the Bryan and Cox model.

Below we briefly review the ocean model equations and the underlying physical assumptions in deriving them. This is done primarily to illustrate how physical processes are parameterised in the models, and (later) to show how changes in these parameters can influence acoustic simulations.

We in fact start with the relevant ocean model equations written in three dimensions, the so-called primitive equations, to explain the underlying physics (Section 3.1). Then we indicate the approximations that are made in solving the equations and in deriving other 3-D formulations, for example the quasi-geostrophic model equations (Section 3.2). We also show how the appropriate equations are obtained in deriving 1-D numerical models of the surface mixed layer (Section 3.3).

3.1 Primitive Equation (PE) Models

The study of ocean dynamics is based on a mathematical description of the time-dependent motion of a relatively thin layer of stratified fluid on a rotating earth. The ratio of horizontal to vertical length scales is of the order 1000:1, and it is important to appreciate that the bulk of the kinetic energy in the oceans is contained in horizontal rather than vertical motions. These motions are governed by conservation laws for mass and momentum, an equation of state, and the laws of thermodynamics.

Predictions of the time-dependent current, temperature and salinity are carried out in primitive equation models using the Reynolds averaged conservation equations for fluid flow on a rotating earth, with three further basic assumptions. Firstly, the Boussinesq approximation is made, in which density differences are neglected except in the buoyancy terms, the validity of the approximation being due to the relatively small variations in density in the horizontal, compared to the vertical direction. Secondly, the equation for the vertical component of motion is reduced to the hydrostatic assumption by the neglect of locally vertical components of acceleration and of the Coriolis effect. The third approximation is that a turbulent viscosity hypothesis is made, in which stresses exerted at scales of motion too small to be resolved by the numerical model grids are

represented as enhanced molecular mixing by the use of 'eddy' coefficients.

With these three approximations, the horizontal momentum equations may be written as

$$\frac{\partial u}{\partial t} + (\underline{u}.\nabla)u = -\frac{1}{\rho_o}\frac{\partial p}{\partial x} + fv + A_H\nabla^2 u + A_V\frac{\partial^2 u}{\partial z^2}, \quad (1)$$

$$\frac{\partial v}{\partial t} + (\underline{u}.\nabla)v = -\frac{1}{\rho_o}\frac{\partial p}{\partial y} - fu + A_H\nabla^2 v + A_V\frac{\partial^2 v}{\partial z^2}, \quad (2)$$

where $\underline{u}$ is the velocity vector $\underline{u} = (u,v)$ and u and v are the horizontal velocity components in the x and y directions, respectively. p is the pressure, ρ_o is the density (assumed constant) and f is the Coriolis parameter given by $f = 2\,\Omega \sin\phi$, where Ω is the earth's rotation and ϕ is the latitude. A_H and A_V are, respectively, the horizontal and vertical eddy viscosity coefficients. ∇ is the vector operator $(\partial/\partial x, \partial/\partial y)$. z is positive vertically upwards.

We note here that the terms $\partial u/\partial t$, $\partial v/\partial t$ are local accelerations and that the terms of the form $(\underline{u}.\nabla)u$, $(\underline{u}.\nabla)v$ are field accelerations. The latter are the advective terms, ie $(\underline{u}.\nabla)u = u\,\partial u/\partial x + v\,\partial u/\partial y$, etc and are non-linear (eg $u\,\partial u/\partial x = {}^1/_2\,\partial u^2/\partial x$). As such, they play an important role in ocean dynamics beyond linear states, eg cross-frontal transfers of momentum.

With the hydrostatic approximation, the vertical momentum equation becomes

$$\frac{\partial p}{\partial z} = -\rho g, \quad (3)$$

where g is gravity and ρ is density.

A fourth approximation is made, that the water is incompressible, giving the continuity equation, which is required in 3-D numerical simulations to solve for w,

$$\frac{\partial u}{\partial x} + \frac{\partial v}{\partial y} + \frac{\partial w}{\partial z} = 0. \quad (4)$$

To obtain an equation for the density ρ, the assumption is made that the temperature, T, and salinity, S, are governed by transport equations in which the sub-gridscale transfers of heat and salt are described by horizontal and vertical eddy diffusion coefficients, K_H and K_V, respectively. The equations for the temperature and salinity may then be written as

$$\frac{\partial T}{\partial t} + (\underline{u}.\nabla)T = K_H\nabla^2 T + K_V\frac{\partial^2 T}{\partial z^2}, \quad (5)$$

$$\frac{\partial S}{\partial t} + (\underline{u}.\nabla)S = K_H\nabla^2 S + K_V\frac{\partial^2 S}{\partial z^2}. \quad (6)$$

Source and sink terms may be added to the right hand sides of equations (5) and (6) to account for any gains or losses of heat or salt. Here, for clarity, these terms have been omitted.

To obtain density, ρ, from S and T, it is necessary to employ an equation of state. According to the problem that it is required to solve, this is done with varying levels of complexity. For example, in 'single tracer' versions of 3-D models, variations in T only might be modelled, with S assumed constant, in which case the density is given by

$$\rho = \rho_o (1 - \alpha T) . \qquad (7)$$

Here ρ_o is a reference density and α is the thermal expansion coefficient. Other simple linear relationships are possible to incorporate the effects of variations in S, and ultimately use can be made of empirically based polynomial expressions for density [25].

In principle, therefore, it is possible to solve equations (1)-(6), and the approprate equation of state (7), for u, v, w, p, S, T and ρ, subject to various boundary conditions.

The Coriolis parameter, f, in equations (1) and (2) is a function of latitude. For global or basin-scale simulations it is usual to write the conservation equations in spherical coordinates [26,27] so as to allow f to vary realistically. However, in limited area simulations, further approximations are possible which enable the equations to be used in Cartesian coordinate form. These are f-plane and β-plane approximations.

In the f-plane approximation the Coriolis parameter is assumed constant in a tangent plane to the earth's surface, and given the value $f = 2\Omega \sin\phi$ for a fixed latitude ϕ_o, usually taken as the centre of the area. In general this will be a reasonable approximation for phenomena of relatively small scale, eg 100 km or so.

For larger areas with ϕ varying over a few tens of degrees, the β-plane approximation is used in which the variation in f is expressed linearly in terms of variations N-S about a fixed value, f_o, at the centre of the area, viz $f = f_o + \beta y$, where β is now a linear coefficient.

Realistic environmental simulations to study low frequency sound propagation at long ranges, and the development of basin-scale ocean forecast systems, require that we account properly for the variations that occur in f. In practice, this means that the relevant equations (1)-(7) are written in spherical coordinates.

3.2 Quasi-Geostrophic (QG) Models

To an order of accuracy of within 1% it is found that, in the interior of the ocean, the resultant horizontal motions are a balance between the pressure gradient terms ($-1/\rho_o\, \partial p/\partial x$, $-1/\rho_o\, \partial p/\partial y$) and the Coriolis terms ($-fu$, fv) (see equations (1)-(2)), while the non-linear terms ($u\, \partial u/\partial x$ etc) and the friction terms ($A_H\, \partial^2 u/\partial x^2$ etc) are negligible by comparison. This geostrophic balance is expressed mathematically, for the x and y components of momentum, in the form $1/\rho_o\, \partial p/\partial x = fv$ and $1/\rho_o\, \partial p/\partial y = -fu$. These equations are diagnostic and cannot be used for predictive purposes. To predict real states, it is necessary to include the local acceleration and advective terms (see above) even though the balance remains primarily geostrophic, viz

$$\frac{\partial \mathbf{u}}{\partial t} + (\underline{\mathbf{u}} . \nabla)\, \mathbf{u} = -\frac{1}{\rho_o} \frac{\partial p}{\partial x} + fv , \qquad (8)$$

$$\frac{\partial v}{\partial t} + (\underline{u} . \nabla) v = - \frac{1}{\rho_o} \frac{\partial p}{\partial y} - fu . \qquad (9)$$

These simplified equations, together with the continuity and hydrostatic equations, and equations for temperature and salinity, form the basis of most QG models.However, it should be noted that QG models that have been developed for predictive purposes, eg the Harvard Open Ocean Model [16], involve solutions to the potential vorticity equation, which is formed by cross-differentiating equations (8) and (9). Further details of this approach are given by Robinson and Walstead [16].

3.3 One Dimensional Formulations

Numerical models have been developed to describe the response of the upper ocean to atmospheric forcing. Because of the disparity in scales between the horizontal dimensions of atmospheric weather systems and the depth of the layer in the ocean through which exchanges take place, most surface mixed layer models are in general 1-D models. In these models horizontal pressure and velocity variations are ignored, and the principal balance is between the accelerative terms in the momentum equations, the vertical flux of horizontal momentum or horizontal shear, and Coriolis. Experimental measurements have confirmed this and show that, over time scales of the order of days, vertical mixing is likely to be the dominant process controlling the distribution of heat in the surface mixed layer. At longer time scales, of the order of weeks, it is necessary to take into account advective effects to obtain a proper heat balance between the atmosphere and the upper ocean.

With these approximations, the equations for conservation of momentum, heat and salt, in the vertical, may be written,

$$\frac{\partial u}{\partial t} = fv + \frac{\partial}{\partial z}\left(A_V \frac{\partial u}{\partial z} \right), \qquad (10)$$

$$\frac{\partial v}{\partial t} = - fu + \frac{\partial}{\partial z}\left(A_V \frac{\partial v}{\partial z} \right), \qquad (11)$$

$$\frac{\partial T}{\partial t} = \frac{\partial}{\partial z}\left(K_V \frac{\partial T}{\partial z} \right), \qquad (12)$$

$$\frac{\partial S}{\partial t} = \frac{\partial}{\partial z}\left(K_V \frac{\partial S}{\partial z} \right), \qquad (13)$$

although, in this case, we note that the eddy coefficients A_V and K_V are no longer independent of z. In principle, having neglected horizontal variations, it would be possible to solve equations (10)-(13) by assigning values to A_V and K_V that are constant and independent of flow conditions. While this approach is found to work reasonably well in 3-D simulations where horizontal or lateral mixing is important, in 1-D models the vertical exchanges become important.For example, vertical mixing may vary as a function of depth and be determined by the characteristics of the flow, in particular the levels of turbulence.

An alternative and more satisfactory approach to solving these equations in the vertical is provided by the 'turbulence closure hypothesis' in which the eddy coefficients A_V and K_V are written in terms of turbulent flow parameters, viz

$$(A_V, K_V) = \lambda q (S_A, S_K) , \qquad (14)$$

where λ is an appropriate length scale for vertical mixing, $q^2/2$ is the turbulent kinetic energy and S_A and S_K are empirical stability functions that depend on the Richardson number (see Pond and Pickard [28] for definition). The length scale λ is obtained from boundary layer theory and the turbulent kinetic energy profile [29,30].

To enable equations in the vertical (10)-(13) to be used for predictive purposes in atmospherically forced simulations, it would be necessary to include a term on the right hand side of (12) to describe heating as a result of penetrating solar radiation, viz $1/\rho c_p \, \partial \Im / \partial z$, where $\Im$ is the downward flux of short wave solar radiation, ρ is density and c_p is specific heat.

With the boundary conditions

$$A_V \left(\frac{\partial u}{\partial z} , \frac{\partial v}{\partial z} \right) \Big|_{z=0} = \frac{1}{\rho_o} (\tau_x, \tau_y) , \qquad (15)$$

$$K_V \frac{\partial T}{\partial z} \Big|_{z=0} = \frac{Q}{\rho_o \, c_p} , \qquad (16)$$

equations (10)-(13), together with an equation of state, are used to solve for u, v and T in many 1-D simulations. Here τ_x and τ_y are the x and y components of the wind stress at the sea surface, and Q is the net heat flux at the sea surface due to long wave radiation, sensible heat and latent heat. Boundary conditions may also be applied to the salinity equation (13) to take account of evaporation and precipitation at the sea surface. In addition it would be necessary to specify the solar radiation at the sea surface.

When tidal mixing is important, ie in shallow water forecast models, it is necessary to incorporate pressure gradient terms, $-1/\rho_o \, \partial p/\partial x$ and $-1/\rho_o \, \partial p/\partial y$, in equations (10) and (11), and to include some frictional damping terms.

1-D mixed layer models in general fall into two categories based on their method of formulation. The first of these are the 'bulk' or 'integrated' models [31,32], in which the mixed layer is assumed to be uniform in temperature and salinity. The governing equations are obtained by integrating equations of the type already described over the depth of the mixed layer. In these models the depth of the mixed layer appears as a diagnostic quantity. These models assume, a priori, the existence of a mixed layer, below which the relevant equations are solved in differential form on a vertical grid.

In the 'continuous' or 'differential' class of models [30,33] the relevant equations are solved in differential form, on a vertical grid over the entire depth. These models therefore give continuous profiles.

Yet another class of models exists, which, although they may be likened to the bulk or integrated models, take a slightly different approach. In these models the 1-D heat conservation equation (12) is used to calculate changes in heat content and potential energy over the vertical. The energy required to 'integrate' these changes over the vertical, so as to achieve a uniform mixed layer, is obtained from wind mixing—the 'mixing' continuing until no further wind energy is available (in

any one time step). Mixing is also achieved as a result of surface cooling and convective stirring, again so as to preserve an energy balance, although in this mechanism some allowance is made for turbulent dissipation.

Such models are known as 'energy balance' models, and in this paper we describe the use of such a model for mixed layer simulations and acoustic considerations.

4. ACOUSTIC MODELS

To determine the sensitivity of acoustic predictions to changes in the modelled environments and in the ocean model parameters, the outputs from the 3-D eddy resolving model described previously have been used as input to acoustic models. Acoustic models have been dealt with at length in other papers in these Proceedings, and several excellent reviews may be found in the literature (eg Harrison [34]). In this study we have used just two models to span a range of frequencies and to represent different features of the acoustic fields. The ray theory model GRASS has been used to obtain results representative of a high frequency situation (1 kHz), and the wave theory model PAREQ was used to investigate a low frequency case (150 Hz). The bulk of the results here, however, relate to acoustic simulations performed with GRASS.

GRASS (Germinating Ray-Acoustic Simulation System) is a range-dependent ray theory model which can generate ray trace diagrams and frequency-dependent propagation loss curves. The primary use of the model in this study has been to investigate the way in which sound propagation paths are influenced by ocean mesoscale variability, and to study the dependence of acoustic predictions on ocean model parameters. Further details of the acoustic model may be found in Cornyn [35] and Harrison [34].

Using Chien and Millero's [36] equation, sound speed was calculated from the temperature field generated by the ocean model together with a constant value of salinity. Smooth profiles were then fitted to these values using a cubic spline to give continuous first and second order derivatives [35]. Linear interpolation was used between the ocean model profiles to obtain estimates at intermediate range steps.

For the ray tracing to study mesoscale perturbations in sound propagation paths through eddy and frontal regions, 11 rays were used with rays being launched at 1° intervals in a range of angles ±5° about the horizontal. Propagation loss was calculated with the ray density increased to obtain convergent solutions in the calculated intensities. This was found to occur with 48 rays per degree for a range of ±15° about the horizontal, giving a total of 1440 rays.

To determine propagation loss characteristics, using GRASS, a phase-independent intensity calculation was performed with a frequency-dependent volume attenuation coefficient given by Thorp's equation [37]. At the ocean surface, rays were assumed to be specularly reflected without attenuation, while for the majority of the investigations the ocean bottom was assumed to be fully absorbing, so as to isolate the acoustic effects of the in-water changes. Experiments were also carried out in which range-dependent bottom loss was added as a lower boundary to the ocean model results.

In all these calculations an omnidirectional sound source has been assumed with the rays confined

between the angular limits given above. The sound source was placed at a depth of 100 m and the receiver at depths of 100 m and 250 m.

To determine the low frequency sound propagation characteristics associated with mesoscale features, we have used the wave theory model PAREQ [34,38,39]. In this case we have performed calculations for a frequency of 150 Hz and with the same source and receiver depth combinations as the GRASS experiments. For these calculations it was necessary to simulate the effects of sound interacting with the ocean bottom and so the model was set up with a 500 m layer of sediment of density 1500 kg m^{-3} and with an attenuation factor of 0.3 dB per wavelength. A seawater to sediment sound speed ratio of 1.003 was used with a sound speed gradient within the sediment layer of 1.3 m s^{-1} per m. This in effect gave a 'high loss' bottom so that the in-water effects of changes in the sound speed field could be studied in the same way that they were in the GRASS simulations. Experiments have also been performed in which other bottom loss conditions have been employed.

5. CASE HISTORIES

The object of this section of the paper is to show how 1-D and 3-D numerical ocean models may be used to study the sensitivity of acoustic predictions to changes in the environment and in the model parameters that are used to predict that environment. This has particular relevance to the design of naval ocean forecast systems [4], where for acoustic purposes it is necessary to achieve accurate and realistic predictions of the ocean environment.

5.1 1-D Considerations

Naval sonar operators require to know the depth of the surface mixed layer or duct. The characteristics of this region of the upper ocean will be influenced primarily by atmospheric forcing. Figure 1 illustrates the changes that may take place over a 15 day period in response to wind mixing and surface heating. These results are in fact a numerical simulation using a 1-D energy balance model (see Section 3.3). Similar trends are observed in the measured profiles of temperature at this location.

We have seen previously that different formulations of the 1-D physics are possible, and Martin [29] has shown that these may lead to quite different characteristics in the vertical profiles through the mixed layer and beneath it. In tests on six models, Martin found that different models predicted different layer depths and temperatures, and different gradients below the layer. How important then are these differences for the acoustics? How accurately do we need to know mixed layer properties for reliable acoustic predictions?

In naval ocean forecast systems employing 1-D synoptic mixed layer modelling schemes, it is necessary to represent the predicted ocean thermal structure, and hence the sound speed profile, at discrete levels in the model. Computational requirements mean that only a limited number of levels are available in the vertical, and that there is an inherent limitation on the accuracy with which the depth of the surface duct can be predicted. This problem is likely to be more accute in 3-D ocean prediction models where the overall requirements of computer memory may give fewer levels in the vertical.

COUPLED OCEAN-ACOUSTIC MODELLING

Following Urick [40], the propagation loss PL in a surface duct, due to geometrical speading and volume attenuation, is given by

$$PL = -5\log\left[\frac{8}{R}\left(1-\frac{d}{H}\right)\right] + 5\log H + 10\log r + (\alpha + \alpha_L)\, r\,, \qquad (17)$$

where d is the source depth, H is the duct depth, r is range, and R is the radius of curvature of the limiting rays in the duct (ie those which are horizontal at the depth H), all in metres. α is now the absorption loss while α_L is the diffraction leakage, both in dB m^{-1}.

Thorp's equation [37] will give α, while α_L is obtained from Shulkin's equation [41]

$$\alpha_L = \frac{1.1\,S}{1000}\left[\frac{F}{H}\right]^{1/2}, \qquad (18)$$

where S is the sea state, and F is frequency in kHz.

Figure 2 shows the variation in propagation loss with changes in duct depth, from equation 17, for an initial isothermal duct of depth 100 m and d/H = 0.5, for ranges of 100, 200, 300 and 400 km. For these calculations, R was set at 90 000 m, frequency at 300 Hz, and sea state at 4. The results show that the errors in PL, for a percentage error in H, are greatest at long range. Typically for moderate sea states and duct depths of about 100 m, the error in PL (at a range of about 200 km) will be ±3 dB for a 10 % error in duct depth.

Table 1 summarises the results of many similar calculations for sea states of 2 and 4, and frequencies of 300 Hz and 2.5 kHz. The table illustrates the order of accuracy that is required in predicting surface duct depths to achieve an accuracy of ±3 dB in the acoustic predictions.

Table 1. Effect of Error in Duct Depth on Propagation Loss.
For a range of 200 km, with the source always at half the duct depth, a change of 3 dB in the propagation loss is caused by the following percentage changes in duct depth:

	Sea State 4			Sea State 2		
Frequency 2.5 kHz	−4 %	100 m	+4 %	−9 %	100 m	+9 %
	−6 %	200 m	+6 %	−12 %	200 m	+14 %
	−7 %	300 m	+8 %	−15 %	300 m	+18 %
Frequency 0.3 kHz	−12 %	100 m	+15 %	−25 %	100 m	+38 %
	−18 %	200 m	+23 %	−34 %	200 m	>50 %
	−21 %	300 m	+31 %	−41 %	300 m	>50 %

In general, from the results shown in Figure 2 and Table 1, we conclude that duct depths need to be known to greater accuracy at higher frequencies, at higher sea states, at longer ranges and for shallower duct depths. In later sections we discuss the implications of these results for the design of naval ocean forecast systems.

5.2 3-D Considerations

We have seen previously that 1-D numerical models may be used to study the sensitivity of acoustic predictions to changes in the surface duct that occur as a result of atmospheric forcing. In reality other features may influence duct depth, in particular ocean eddies (Figure 3) and fronts. To study these features we need 3-D numerical ocean models.

To address this problem we have used an adaptation of the Cox model [42]. The model is configured so as to represent an idealised frontal system in a 3-D rectangular flat bottomed ocean domain with temperature contrasts and physics appropriate to the polar front east of Iceland—the Iceland-Faeroes Front. The set-up is shown in Figure 4 which is a 3-D view of the front at 8 days following an initial baroclinic disturbance at the front (see later).

Following Cox, the equations for the conservation of heat, salt and momentum are written with Boussinesq, hydrostatic and rigid lid approximations, in spherical polar coordinates. The equations are solved in finite difference form on an Arakawa B-grid and with a leap-frogging time stepping scheme [43]. The Coriolis term is treated semi-implicitly so as not to resolve inertial oscillations in time. The frictional terms $A_H \nabla^2 \underline{u}$ (see equations (1-2)) are lagged by one time step for numerical stability. A forward time step is taken every 20 time steps to avoid a computational mode arising from the leap-frog scheme. The barotropic stream function is solved by successive over relaxation.

The Cox model is used in preference to other models, eg quasi-geostrophic models [16,44] and isopycnal coordinate models [24], because it is a robust and well understood model, and is widely used in the ocean modelling community in the UK.

The model is set up with 15 levels in the vertical, with $\Delta z = 25$ m in the top two levels and with $\Delta z = 75$ m in the remaining 13 levels, giving a total depth of 1025 m. The horizontal range increments are $\Delta x = \Delta y = 5$ km, with a total of 72 grid boxes in the x and y directions, giving overall dimensions of 360 km x 360 km. The time step used for these particular simulations was $\Delta t = 360$ s. For the bulk of the simulations described here, the horizontal and vertical eddy viscosity coefficients, A_H and A_V, were set to 10^7 and 1 $cm^2 s^{-1}$, respectively, while the horizontal and vertical eddy diffusion coefficients, K_H and K_V, were set to 10^5 and 1 $cm^2 s^{-1}$. However, for the acoustic investigations that follow, A_H and K_V have also been varied within a range of values representative of ocean model studies elsewhere.

To obtain the results that are described here, the model was initialised with an east-west front having a temperature difference across the front of approximately 3.3 °C to correspond to the Iceland-Faeroes Front. The front is in fact a two-layer representation of warm North Atlantic water meeting and overlying cold Norwegian Sea water. The thickness of the upper, warmer, layer increases asymptoticaly away from the front to a mean depth of 500 m. Boundary conditions in the E-W direction are cyclic, and in the N-S direction may be closed or open. In the latter case, open boundary conditions are applied using the method due to Stevens [45]. Since the flow in these experiments is essentially zonal (from west to east), the results of simulations with N-S boundaries open are not significantly different from those with the boundaries closed.

The model will in fact evolve its own current field to give a geostrophically balanced frontal jet. To save time in the simulation, however, an initial current field is computed for the model by converting the initial temperature distribution into density, assuming constant salinity, and then integrating this in the thermal wind equation.

In this study, the model has been used to generate eddies by introducing a baroclinic perturbation over a region of the front. This was achieved by increasing the temperature by 1 °C in the top 300 m of the water column along a 55 km section of the front centred on x = 75 km. The model was then integrated forward in time to generate eddy like features at the front (Figure 5). Eddies may also be generated by applying a barotropic perturbation at the front [46].

Two further techniques may be employed to perturb the otherwise geostrophically stable front. A sinusoidal perturbation of arbitrary wavelength and amplitude may be imposed on the front or a discrete eddy like feature may be inserted in the modelled fields in close proximity to the front. Following Kielmann and Kase [47] and Smith and Davies [48], this has been achieved by introducing a temperature anomaly of the form

$$\Delta T = \frac{A}{\cosh^2(z/D)} \exp\left[\frac{-\{(x-x_c)^2 + (y-y_c)^2\}}{2L^2}\right]. \qquad (19)$$

Here A is the amplitude (°C) of the eddy, D is a vertical depth scale (typically of the order 200 m), (x_c, y_c) is the horizontal position (longitudinally, latitudinally) of the centre of the eddy. L is the e-folding width scale of the eddy, and is of the order of the first internal Rossby radius of deformation R_i [28], given by

$$R_i = \frac{1}{f}\left[\frac{g(\rho_2 - \rho_1)h}{\rho_2}\right]^{1/2}, \qquad (20)$$

ρ_1 and ρ_2 being the densities of the upper and lower layers in the frontal simulation, g is gravity, h is the depth of the upper layer, and f is the Coriolis parameter. For this study, R_i is about 15 km and L has been set to R_i. Further details of the eddy initialisation are given later.

For the bulk of the acoustic investigations we have concentrated on a section through the front at x = 120 km and a section parallel to the front at y = 200 km. Eddy features may be placed anywhere in the modelled domain, and Figure 6 shows the resulting near-surface temperature field at 16 days after initialisation with a cyclonic cold core eddy placed to the south of the front on the section at x = 120 km.

It should be noted that in the context of this study, the ocean model is used as a process model. The model has no external forcing, ie it is not forced by wind stress at the sea surface and the model does not have a thermodynamically active surface layer. For the purposes of the acoustic investigations that are described here, the model is used purely as a 'generator' of mesoscale frontal and eddy environments for input to acoustic models. The use of an atmospherically forced ocean model to provide comparable simulations is being investigated elsewhere. Further details of the the ocean model are given in [4,46,49].

The results of frontal simulations with the model are shown in Figures 4-8. Figure 4 illustrates the 3-D structure of the front at 8 days after the initial baroclinic disturbance, while Figure 5 shows the

near-surface temperature fields at 0, 2, 4 and 8 days. These results indicate a wave-like disturbance spreading towards the east which after 8 days has the characteristic backward breaking wave appearance typical of these features in numerical model simulations [50] and in satellite images of the Iceland-Faeroes Front region [51]. Figure 5a illustrates the initial baroclinic disturbance used to generate these features.

The eddy structure of the front becomes more apparent at longer integration periods. Figure 7 shows the situation at 24 days, with non-linear cross-frontal processes giving rise to detached eddy features. This is indicated by the closed or nearly-closed nature of the circulation paths in the simulated ocean currents. Henrick et al [52] have shown that the latter may be important in causing horizontal sound refraction effects. Such effects are relatively easy to study in 3-D ocean model simulations of the type described here.

Temperature sections through and along the front at 8 days are shown in Figure 8. It should be noted that although in the along-front (E-W) section the thermal structure gives the appearance of detached or isolated eddy features, these distributions are in fact produced by relatively small N-S displacements of the front. Since in this study we are only able to consider sound propagation in two dimensions, we shall in future refer to these features as 'eddy-like features'.

Figure 8b illustrates the classic two-layer structure of the front which, as explained earlier, could correspond to warm North Atlantic water overlying cold Norwegian Sea water at the Iceland-Faeroes Front [53]. It should be noted that in these simulations we have no representation of bottom topography, so the effects of the Iceland-Faeroes ridge in modifying the frontal structures have not been simulated. Hallock [53] showed that the deep thermal structure is modified by the ridge, giving rise to a cold water overflow region at depth.

In this two-layer representation of the front there is little vertical structure because none was present in the initial profiles. Measurements in the Iceland-Faeroes Front region [51] reveal considerable small scale structure, due to internal waves and turbulence, that cannot be reproduced in the model simulations described here. The acoustic significance of this detail is being investigated elsewhere. However, to first order, we would expect these effects to give rise to perturbations in the sound speed field that are an order of magnitude smaller than those which occur as a result of mesoscale variability.

Figures 9 and 10 illustrate the results of ray tracing on the sections through and along the front (see Figure 4), with the sound source placed at a depth of 100 m at opposite ends of the sections. Figure 9a shows that, with the sound source placed in the warm water to the south of the front, sound energy travels deep in a surface duct as far as the front. There it is refracted downwards into the colder and acoustically slower water to the north. With the source to the north (Figure 9b), it can be seen that the sound energy is generally unable to penetrate the warm layer and is refracted beneath it.

Figure 10 clearly illustrates the effect of mesoscale features on sound propagation, showing sound energy deflected downwards by as much as 300 m beneath the eddy-like features illustrated in Figure 8a. These features, which in 2-D are equivalent to warm-core eddies, have a sound speed change of about 10 m s^{-1} associated with them. From Figure 10 we see that, when considering the eddy-like features, the changes to the sound propagation paths are broadly similar in the E-W direction and the W-E direction.

Coupled ocean-acoustic models also enable the temporal variations in the acoustic effects of frontal regions to be studied. For the baroclinic perturbation case, we have found that the through-front propagation characteristics are hardly altered in the early stages of frontogenesis. For periods out to 8 days the only observed change was a gradual broadening of convergence zones (CZs) which appear in the cold water to the north of the front when the sound source is to the south (Figure 9a). This is associated with a weakening of the cross-frontal temperature gradients on this section (ie x = 120 km) as the front eveolves. At other locations these gradients might actually be strengthened, giving rise to different propagation characteristics. Few other generalisations are possible at this stage regarding CZ characteristics because we have assumed a fully absorbing bottom for rays striking the seabed.

In contrast, sound propagation in directions parallel to the front (eg y = 120 km) show a great deal of variability as the front evolves from its initial linear state. These changes are not surprising as only relatively small displacements of the front are required to induce large changes in the along-front temperature and sound speed fields. The observed changes in sound propagation paths will also depend critically on where the section is taken in relation to the front. In general, perturbations in the sound speed field and the sound propagation characteristics will be greatest when the displacement due to mesoscale frontal features is normal to the sound propagation path.

Corresponding to the temperature sections shown in Figure 8, propagation loss curves were calculated with GRASS for a frequency of 1 kHz (see Section 4). Source/receiver depth combinations of 100/100 m and 100/250 m were used, the latter to illustrate the differences that occur with the receiver placed below the general level of mesoscale disturbance. For both the cross-front (x = 120 km) and through-front (y = 200 km) cases, a range-independent propagation loss curve was also calculated by assuming uniform conditions down range based on the first profile in the modelled section. The results of these calculations are shown in Figure 11a, for a source/receiver depth combination of 100/100 m only.

With the model integrated to 8 days, the most striking feature of the through-front propagation is the 15 dB average propagation loss which occurs with the source at a depth of 100 m as the sound travels from the warm to the cold side of the front. Beyond this, fluctuations of about ±10 dB occur as a result of the CZ behaviour described previously (see Figure 9a). With the receiver at 250 m, Figure 11a shows that the frontal effect is less pronounced but still equivalent to about 5 dB.

For the section along the front at y = 200 km, Figure 11b shows a 20 dB increase in propagation loss, relative to the range-independent case, which is associated with eddy-like features at the front. With the receiver at 250 m, the effect of the eddies is less pronounced although there is an overall shift downwards in the propagation loss curves.

6. DISCUSSION

Ocean forecast systems that are being developed for navy operational use will be required to give accurate and reliable environmental simulations for input to range-dependent acoustic models and to meet other operational requirements, eg search and rescue, pollution control, etc. In designing such systems it is important that we have a proper awareness of the limitations placed on ocean models by these requirements and by the availability of computer power.

Restricted computing power may result in limited spatial and temporal resolution in forecast models. What will be the effect of this on acoustic accuracy? Restrictions on communications may require the use of data compression techniques, with a consequent loss of detail in the predictions. Again, the question arises of what the effect will be on acoustic simulations.

In the following sections we elaborate on the case histories outlined previously to show how the coupled ocean-acoustic modelling technique may be used as a design aid in the development of operational ocean forecast systems. In particular, we discuss the results of 1-D and 3-D ocean-acoustic sensitivity studies to address the twin problems of accuracy and resolution.

6.1 1-D Results

For naval ocean forecast systems employing 1-D synoptic mixed layer modelling schemes (eg US Navy's TOPS [11] and the Royal Navy's NEAT MLM [4]), it is necessary to achieve an optimum distribution of levels in the vertical for consistent acoustic accuracy. In the NEAT MLM system, developed by the Admiralty Research Establishment, this is achieved by distributing the model levels to give a constant 10 % depth resolution over a range of duct depths. As shown in Section 5.1, this corresponds typically to a ±3 dB uncertainty in the acoustic predictions at moderate sea states and medium ranges.

The results in Figure 1 show that failure to take account of changes in the surface mixed layer occuring as a result of atmospheric forcing may lead to gross errors in surface duct predictions. Simulations of the type shown in Figure 1 suggest that actual duct depths may differ by as much as 20 to 30 % from those expected on the basis of climatology, possibly leading to errors as large as 10 dB.

Figure 1 also clearly demonstrates the importance of near-surface temperature gradients resulting from surface heating. Porter et al [12] have shown that these can be crucial in acoustic predictions. Hence the usefulness of 1-D ocean-acoustic simulations in which mixed layer model parameters can be varied.

Operationally, the information generated by the NEAT MLM system on the thermal structure of the upper ocean for, say, 200 locations over the NE Atlantic has to be reduced to a manageable size for the purposes of naval communications. This is achieved by reducing individual profiles to 'break-points'. However, this process can induce further uncertainty by misrepresenting layer depth. 1-D ocean-acoustic simulations can help in studying this problem by performing sensitivity tests with various break-pointing algorithms.

A typical algorithm splits a continuous temperature profile into a series of straight lines, where the lines are as long as possible without deviating by more than 0.15 °C from the actual profile. Only the end coordinates of the lines then need to be transmitted, reducing the burden on communications. However, this algorithm will almost inevitably result in an isothermal layer being represented by a surface duct with a temperature gradient of $0.15/H$ °C m^{-1}, where H is the duct depth. An overestimate of H by 10% is another typical result of the break-pointing (this result depends on the depth resolution of the original temperature profile). Equations (17) and (18) can be used to find the dependence of PL on variations in thermal gradient and duct depth of this order of magnitude. The gradient affects PL by changing R, the radius of curvature of the limiting rays propagating in the duct. Over a range of 100 km, the break-pointing algorithm changes the predicted propagation loss by 1 to 1.5 dB for a sea state of 4 and a frequency of 300 Hz [54].

These results indicate that the depth resolution of a 1-D ocean model does not need to be better than about 5% if the resultant temperature profiles are compressed by break-pointing. This resolution, while not achieved by present operational systems, is well within the capability of modern serial computers.

Other tests are possible using 1-D models to study acoustic sensitivity in relation to ocean model parameters (eg those decribing mixing and heat up-take in the ocean—see Section 3.3) and atmospheric forcing (eg optical properties of sea water).

6.2 3-D Results

The results of this study have demonstrated the versatility of the coupled ocean-acoustic modelling technique in being able to provide high resolution environmental data sets, with simulated mesoscale variability, for input to range-dependent acoustic models.

A particular advantage of this technique is that it is possible to perform ocean-acoustic simulations under well controlled conditions, varying the acoustic model parameters (eg frequency, source depth) within experimentally and operationally useful ranges, and introducing spatial and temporal variability into the problem in a way that would be difficult to achieve with measurements alone. The environmental data sets are also synoptic, overcoming the difficulty that is experienced in measurements at sea where mesoscale features may evolve on time scales comparable to those that are required to survey them.

Measurements at sea can also be costly and time consuming. While observations are important in improving our understanding of basic processes in the ocean, and their parameterisation in ocean models, computer models provide a cost effective means of studying mesoscale acoustic variability.

However, this requires us to have conviction in the ocean model results. Forecast models (eg Melberg et al [14]) are initialised and constrained by oceanographic and other data, eg satellite observations of frontal meanders and eddies. On the other hand, verification of process models relies on comparisons with theoretical predictions which give maximum growth rates for preferred wavelengths, according to mesoscale frontal dynamics.

For the situation described here, tests were performed by applying a small amplitude sinusoidal perturbation at the front and comparing the observed rates of growth of features having different wavelengths with those predicted by linear theory of Killworth et al [55]. The latter predict maximum growth rate to be at a wavelength given by $2\pi R_i$ where R_i is the internal Rossby radius (equation 20). For the present study, with h = 500 m, ρ_1 = 1027.10 kg m^{-3} and ρ_2 = 1027.92 kg m^{-3}, we obtain $R_i \approx 15$ km, corresponding to a wavelength $2\pi R_i$ = 94 km. The observed growth rates agreed well with those obtained by Killworth et al [55], with all non-zero growth rates lying within 11 % of their results. Further details of these tests are given in [56].

Comparisons were also made with the observed wavelengths of the features generated by the baroclinic perturbation technique described previously. These tests showed that with the model integrated to 8 days, beyond which the frontal dynamics becomes highly non-linear, the observed wavelengths of frontal features lay within a range 90 to 120 km, and therefore close to the figure of 94 km given by linear theory.

While these tests have confirmed that realistic mesoscale simulations may be possible with numerical ocean models, they do not provide evidence that the simulated environments will be suitable for acoustic purposes. In particular, it is possible to perform simulations that are dynamically correct and which give realistic spatial and temporal scales for the observed features but which may contain significant differences in detail. In large measure these differences will be due to our choice of ocean model parameter values, in particular those values which describe mixing processes that are too small to be resolved by the numerical model grids. For naval ocean forecast system design it is important that we know precisely how significant these differences are acoustically.

To address this problem we have performed numerical simulations in which the horizontal eddy viscosity parameter A_H was varied in the range 0.1 to 2 x 10^7 cm^2 s^{-1}. A_H is approximately two orders of magnitude larger than the next largest eddy parameter, the horizontal eddy diffusion coefficient K_H, which is of the order 10^5 cm^2 s^{-1}. The remaining coefficients, A_V and K_V, are of order 1 cm^2 s^{-1}. In these experiments the model was initialised with the same baroclinic disturbance. Figure 12 shows the results of these comparisons, with the model integrated to 8 days, and illustrates that with A_V, K_H and K_V constant, the lowest value of A_H (Figure 12a) gives noisy results, while the largest value (Figure 12d) gives results in which the growth rate is reduced, although the spatial scales are similar. A similar study was carried out in which K_H was varied in the range 0.1 to 2 x 10^5 cm^2 s^{-1}, and this showed (Figure 13) that there was little discernable difference in the modelled fields at 8 days.

The effect of the choice of A_H in equations (1) and (2) can be seen if we consider the effect of the eddy viscosity term in the simplified momentum equation

$$\frac{\partial u}{\partial t} = A_H \frac{\partial^2 u}{\partial x^2}, \qquad (21)$$

where u is the horizontal velocity in the x direction. By inspection equation (21) gives a relation between length (L) and time (T) scales of the form $T = L^2 / A_H$, where L is now a length scale associated with the size of a feature and T is a time scale for its decay (as a result of momentum diffusion).

Thus, with $A_H = 10^7$ cm^2 s^{-1}, equation (21) gives a characteristic 'spin-down' time for an ocean eddy of diameter $2R_i$ = 30 km of about 16 days. This is longer than the time scales of interest in operational ocean forecast models, and suggests that with suitable data assimilation schemes it will be possible to predict this level of detail in mesoscale simulations. However, the question remains as to the acoustic significance of the detailed changes that are shown in the ocean model simulations at Figure 12. To assess this problem we have performed propagation loss calculations on the sections described previously, both through and along the front, for a range of A_H values.

Tests have been performed with the acoustic ray theory model GRASS, to give a representative high frequency (1 kHz) case. The results of the calculations with GRASS are shown in Figure 14. They suggest that for sound propagating through the front (Figure 14a) there will be an uncertainty of ±5 dB associated with the in-water differences due to the different eddy viscosity values. However, for the sound propagating parallel to the front, the variations are of the order ±10 dB. In the latter case, the effects are particularly noticeable at short ranges, ie out to about 40 km. Figure 15 shows acoustic ray traces from model simulations performed with A_H set at 0.1 x 10^7 cm^2 s^{-1}

and 0.5 x 10^7 cm^2 s^{-1}, for the same initial disturbance to the front and with the model integrated for 8 days. The differences at short range (< 40 km) are very apparent, although it should be noted that there are significant differences in the sound propagation paths at long range also. Clearly these differences will depend on the location of the sound source in relation to the ocean feature. However, the range of A_H values that has been studied here is similar to that used in other ocean model simulations (eg Dippner [50] used A_H = 0.3 x 10^7 cm^2 s^{-1}) and suggests that the acoustic calculations at this frequency will be sensitive to eddy viscosity in the ocean model. These effects are discussed in greater detail by Heathershaw et al [49].

Similar comparisons have yet to be carried out with PAREQ. However, the early indications are that despite the lower frequencies, in-water effects are still important and that the acoustic predictions may still be sensitive to ocean model parameters. Figure 16 shows propagation loss curves calculated with PAREQ for the section along the front at y = 200 km and through the eddy-like features shown in Figure 8a, but for the model integrated to 2 days and 8 days. These results clearly indicate the temporal variability in propagation loss due to the changes occurring in the simulated mesoscale environment, even at low frequencies.

7. CONCLUSIONS

Simulations with a 1-D mixed layer model demonstrate that daily variations in the surface duct can now be predicted with a simple numerical model incorporating atmospheric forcing. Calculations of the effect of small changes in the surface duct on propagation loss have shown the importance of using realistic ocean forecast models to obtain accurate sonar performance predictions.

Studies with a 3-D eddy resolving ocean model being used to provide simulated mesoscale environments for input to range-dependent acoustic models have demonstrated the versatility of the coupled ocean-acoustic modelling technique. Insight is provided into the sensitivity of acoustic predictions to changes in the modelled environments and in model parameter values.

In particular, we have found that acoustic predictions at high frequencies (of order 1 kHz) are sensitive to ocean model parameter settings, in particular the horizontal eddy viscosity coefficient. At low frequencies (of order 150 Hz) we find that the acoustic predictions are less sensitive to the in-water changes that occur as a result of the different eddy viscosity values, although, on the basis of the limited set of comparisons carried out here, it is still necessary to take account of these differences.

8. ACKNOWLEDGEMENTS

We are grateful to present and former colleagues in the Ocean Science Division at ARE Portland for their assistance in the preparation of this paper. James Martin, Lopez Shackleford and Gary Pavey assisted with the 1-D modelling work. Steve Maskell of Exeter University, Bill Cooper and Claire Mooney carried out the simulations with the 3-D ocean model. Roger Hillman has provided invaluable guidance on the use of acoustic models. Davie Barr of the Computer Support Group at ARE is also thanked for his unstinting efforts in overcoming computer problems.

9. REFERENCES

[1] Semtner, A. and Chervin, R. (1988a). 'Breakthroughs in ocean and climate modelling made possible by supercomputers of today and tomorrow', Proceedings of Supercomputer '88 Conference, Vol II, Science and Applications, 230-239.

[2] Semtner, A. and Chervin, R. (1988b). 'A simulation of the global ocean circulation with resolved eddies', J. Geophys. Res., 93, 15502-15522.

[3] Clancy M. (1987). 'Real-time applied oceanography at the Navy's Global Center', Mar. Tech. Soc. Journal, 21, 33-46.

[4] Heathershaw, A. D., Gething, M. R. and Foreman S. J. (1990a). 'Ocean forecast models for ASW', Proceedings, Underwater Defence Technology Conference, London, 123-128.

[5] Henrick, R. F., Siegmann, W. L. and Jacobson, M. J. (1977). 'General analysis of ocean eddy effects for sound transmission applications', J. Acoust. Soc. Am., 62, 860-870.

[6] Henrick, R. F., Jacobson, M. J. and Siegman, W. L. (1980). 'General effects of currents and sound speed variations on short range acoustic transmission in cyclonic eddies', J. Acoust. Soc. Am., 67, 121-134.

[7] Baer, R. N. (1981). 'Propagation through a three-dimensional eddy including the effects on an array', J. Acoust. Soc. Am., 69, 70-75.

[8] Rousseau, T. H., Siegmann, W. L. and Jacobson, M. J. (1982). 'Acoustic propagation through a model of shallow fronts in the deep ocean', J. Acoust. Soc. Am., 72, 924-936.

[9] McManus J. J. (1985). 'Coupled mixed layer-acoustic model', Master's Thesis, Naval Postgraduate School, Monterey, California, USA.

[10] Fourniol, J. M. (1987). 'Coupled acoustic and ocean thermodynamic model', Master's Thesis, Naval Postgraduate School, Monterey, California, USA.

[11] Clancy, M. and Pollack, K. (1983). 'A real-time synoptic ocean thermal analysis/forecast system', Prog. Oceanog., 12, 383-424.

[12] Porter, M., Piacsek, S., Henderson, L. and Jensen, F. (1989). 'Acoustic impact of upper ocean models', unpublished manuscript, SACLANT Undersea Research Centre.

[13] Botseas, G. and Seigmann, W. L. (1989). 'IFD: Interfaced with Harvard Open Ocean Model forecasts', Naval Underwater Systems Center, Connecticut, Technical Report 8367.

[14] Melberg, L. E., Robinson, A. R. and Botseas, G. (1990). 'Modeled time variability of acoustic propagation through a Gulf Stream meander and eddies', J. Acoust. Soc. Am., 87, 1044-1054.

[15] Lee, D. and Botseas. G. (1982). 'IFD: An Implicit Finite Difference computer model for solving the parabolic equation', Naval Underwater Systems Center, Connecticut, Technical Report 6659.

[16] Robinson, A. R. and Walstad, L. J. (1987). 'The Harvard Open Ocean Model: Calibration and application to dynamical process, forecasting and data assimilation studies', Applied Numerical Mathematics, 3, 89-131.

[17] Bryan, K. (1969). 'A numerical method for the study of the circulation of the World Ocean', J. Comp. Phys., 4, 347-376.

[18] Semtner, A. (1984). 'An oceanic general circulation model with bottom topography', UCLA Dept. of Meteorology Tech. Report No. 9, 99pp.

[19] Bryan, K. and Cox, M. (1967). 'A numerical investigation of the ocean general circulation', Tellus, 19, 54-80.

[20] Takano, K. (1974). 'A general circulation model for the World Ocean', UCLA Dept. of Meteorology Tech. Report No. 8.

COUPLED OCEAN-ACOUSTIC MODELLING

[21] Holland, W. R. and Lin, L. B. (1975). 'On the generation of mesoscale eddies and their contribution to the oceanic general circulation. I. A preliminary numerical experiment', J. Phys. Oceanogr., 5, 642-657.
[22] Haidvogel, D. B., Robinson, A. R. and Schulman, E. E. (1980). 'The accuracy, efficiency and stability of three numerical models with application to ocean problems', J. Comp. Phys., 34, 1-53.
[23] Pedlosky, J. (1979). *Geophysical Fluid Dynamics*, Springer-Verlag, 624pp.
[24] Bleck, R. and Boudra, D. B. (1986). 'Wind driven spin-up in eddy-resolving ocean models formulated in isopycnic and isobaric coordinates', J. Geophys. Res., 91C, 7611-7621.
[25] Millero, F. J. and Poisson, A. (1981). 'International one-atmosphere equation of state of sea-water', Deep-Sea Res., 27A, 255-264.
[26] Apel, J. R. (1987). *Principles of Ocean Physics*, Academic Press, 605pp.
[27] Washington, W. M. and Parkinson, C. L. (1986). *An Introduction to Three Dimensional Climate Modelling*, Oxford University Press, 422pp.
[28] Pond, S. and Pickard, G. L. (1983). *Introductory Dynamical Oceanography*, Pergamon Press, 319pp.
[29] Martin, P. J. (1985). 'Simulation of the mixed layer at OWS November and Papa with several models', J. Geophys. Res., 90, 901-916.
[30] Mellor, G. L. and Yamada, T. (1974). 'A heirachy of turbulence closure models for planetary boundary layers', J. Atmos. Sci., 31, 1791-1806.
[31] Garwood, R. W. (1977). 'An oceanic mixed layer model capable of simulating cyclic states', J. Phys. Oceanog., 7, 455-468.
[32] Niiler, P. P. (1975). 'Deepening of the wind-mixed layer', J. Mar. Res., 33, 405-422.
[33] Mellor, G. L. and Yamada, T. (1977). 'A turbulence model applied to geophysical fluid problems', Proc. Symp. on Turbulent Shear Flows, Pennsylvania State University, University Park, Pa., USA, April 1977, 1-14.
[34] Harrison, C. H. (1989). 'Ocean propagation models', App. Acoust., 27, 163-201.
[35] Comyn, J. (1973). 'GRASS: A digital-computer ray-tracing and transmission loss prediction system. Vol 1 - Overall description', Naval Research Laboratory Report, 7621.
[36] Chien, C. T. and Millero, F. J. (1977). 'Speed of sound in sea water at high pressures', J. Acoust. Soc. Am., 62, 1129.
[37] Thorp, W. H. (1965). 'Deep-ocean sound attenuation in the sub- and low- kilocycle-per-second region', J. Acoust. Soc. Am., 38, 648-654.
[38] Jensen, F.B. and Kroll, H.R. (1975). 'The use of the parabolic equation method in sound propagation modelling', Report No. SM-72, SACLANT ASW Centre, La Spezia, Italy.
[39] Tappert, F.D. (1977). 'The parabolic approximation method', In *Wave Propagation and Underwater Acoustics*, Ed. J.B. Keller and J.S. Papadakis, Springer-Verlag, Berlin, 224-287
[40] Urick, R. J. (1982). *Principles of Underwater Sound*, McGraw-Hill, 423pp.
[41] Schulkin, M. (1968). 'Surface coupled layers in surface sound channels', J. Acoust. Soc. Am., 44, 1152.
[42] Cox, M. D. (1984). 'A primitive equation, 3-dimensional model of the ocean', GFDL Ocean Group Tech Report No 1, Princeton University.
[43] Arakawa, A. and Lamb, V. R. (1977). 'Computational design of the basic dynamical processes of the UCLA general circulation model', Methods in Comp. Phys., 16, 173-265.
[44] Marshall, J. C. and Nurser, A. J. G. (1986). 'Steady free circulation in a stratified quasi-geostrophic ocean', J. Phys. Oceanog., 16, 1799-1813.

[45] Stevens, D. P. (1990). 'On open boundary conditions for three dimensional primitive equation ocean circulation models', Geophys. Astro. Fluid Dyn., 51, 103-133.
[46] Heathershaw, A. D., Maskell, S. J., Cooper W. St J. and Hillman, R. C. (1988). 'Studies of sound propagation through a front using an eddy resolving ocean model', Admiralty Research Establishment Tech. Memo (UJO) 88144.
[47] Kielmann, J. and Kase, R. H. (1987). 'Numerical modelling of meander and eddy formation in the Azores Current frontal zone', J. Phys. Oceanog., 17, 529-541.
[48] Smith, D. C. and Davies, G. P. (1989). 'A numerical study of eddy interaction with an ocean jet', J. Phys. Oceanog., 19, 103-133.
[49] Heathershaw, A. D., Stretch, C. E. and Maskell, S. J. (1990b). 'Coupled ocean-acoustic model studies of sound propagation through an ocean front', J. Acoust. Soc. Am., (submitted).
[50] Dippner, J. W. (1990). 'Eddy-resolving modelling with dynamically active tracers', Cont. Shelf Res., 10, 87-101.
[51] Scott, J. C. and McDowall, A. L. (1990). 'Cross-frontal jets near Iceland: In-water, satellite infra-red and GEOSAT altimeter data', J. Geophys. Res., to appear.
[52] Henrick,R. F., Jacobson, M. J. and Siegmann, W. L. (1980). 'General effects of currents and sound speed variations on short range acoustic transmission in cyclonic eddies', J. Acoust. Soc. Am., 67, 121-134.
[53] Hallock, R. (1985). 'Variability of frontal structure in the southern Norwegian Sea', J. Phys. Oceanog., 15, 1245-1253.
[54] Gething, M. R. (1990). 'The effect on acoustic predictions of break-pointing temperature profiles', Admiralty Research Establishment Tech. Memo (in preparation).
[55] Killworth, P. D., Paldor, N. and Stern, M. E. (1984). 'Wave propagation and growth on a surface front in a two-layer geostrophic current', J. Mar. Res., 42, 761-785.
[56] Wood, R. A. (1988). 'Instability of oceanic fronts', Ph.D Thesis, University of Exeter, UK.

COUPLED OCEAN-ACOUSTIC MODELLING

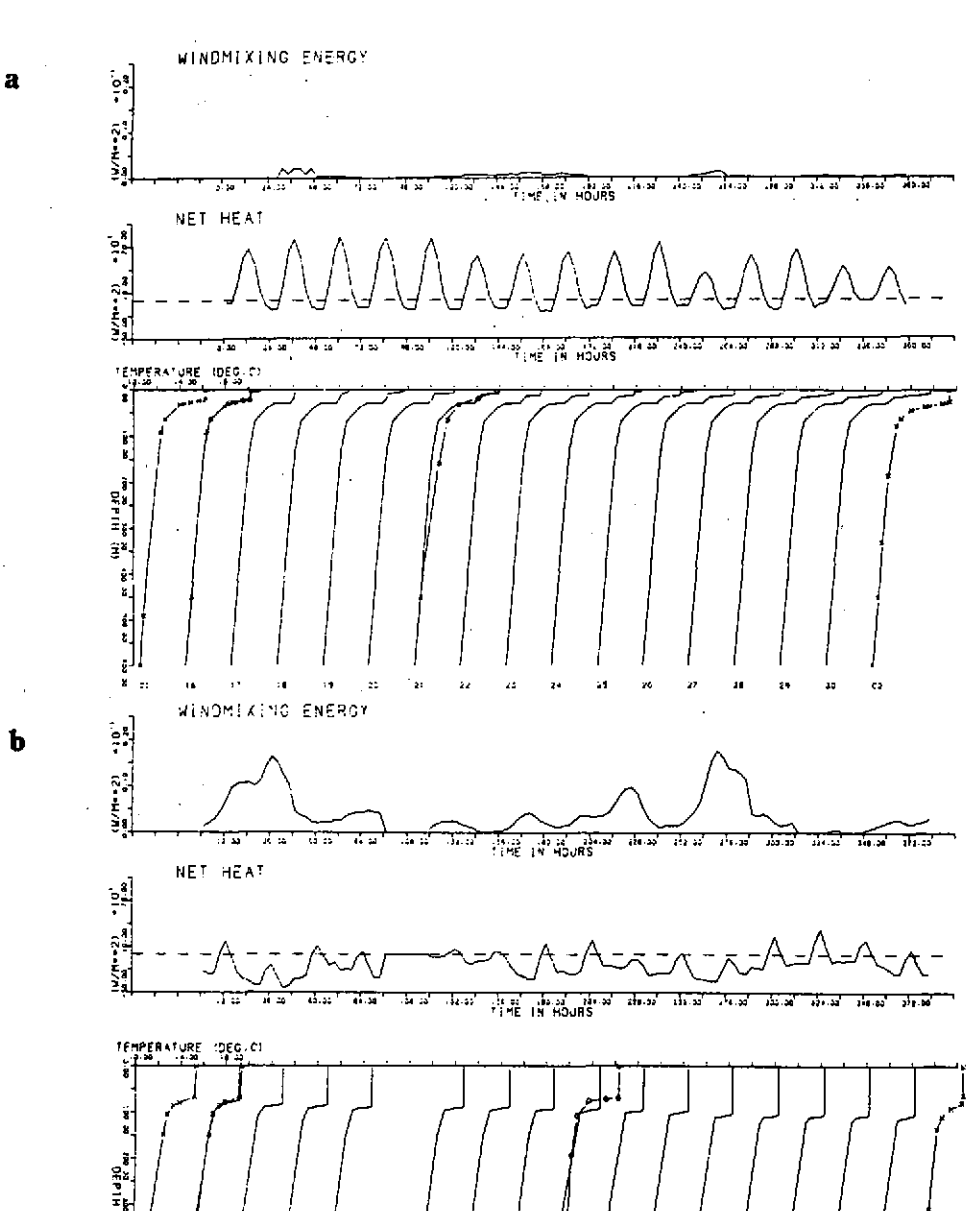

Figure 1. Two 15-day simulations of the surface layer using atmospheric fluxes to drive a mixed layer model, for (a) 16-30 June and (b) 1-16 November 1989. Wind mixing energy and net heat are shown above the temperature-depth profiles. C1 is the climatology profile used to initialise a simulation, while C2 is the climatology profile corresponding to the end of the run. Profiles marked with circles are operational forecasts based on observations. (No fluxes were available for 5 November 1989).

COUPLED OCEAN-ACOUSTIC MODELLING

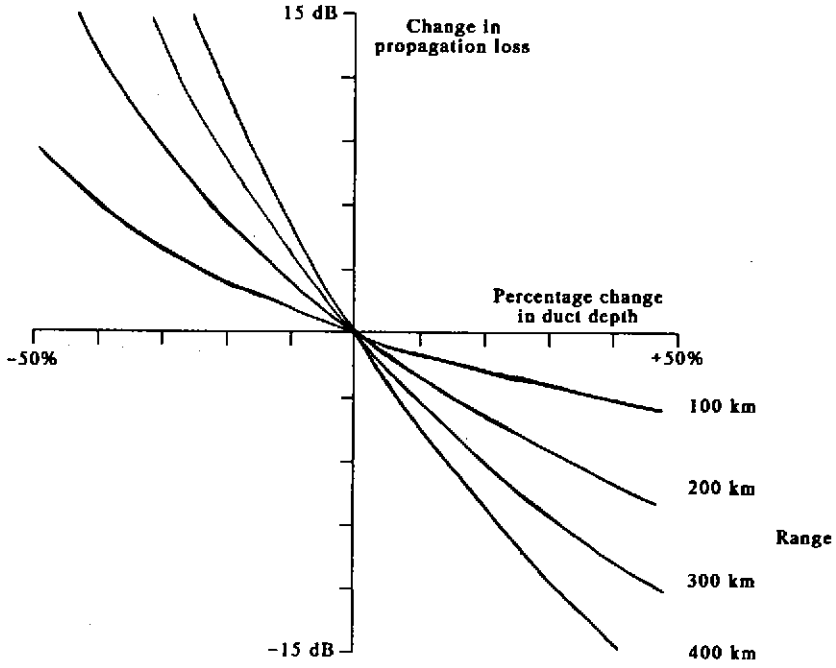

Figure 2. Change in propagation loss in a surface duct, at various ranges, as the duct depth is varied about a mean value of 100 m. Source set at half the duct depth, with a frequency of 300 Hz and sea state 4.

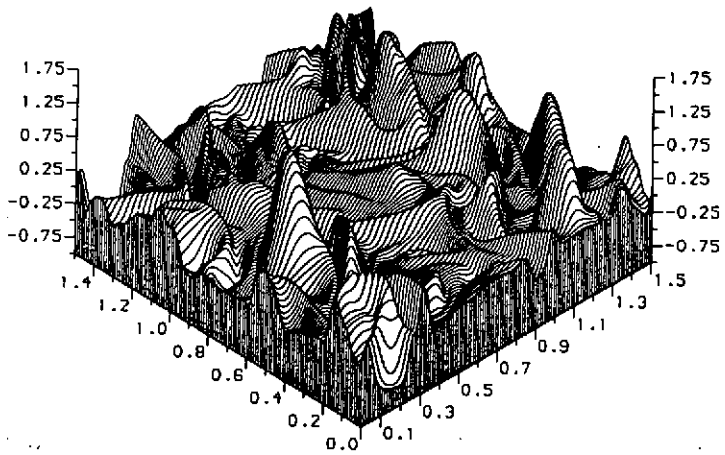

Figure 3. 3-D simulation to show effect of mesoscale eddies on depth of mixed layer. x and y axes show ranges 0 to 1500 km, z axis shows depth anomaly from −10.0 to +17.5 m.

COUPLED OCEAN-ACOUSTIC MODELLING

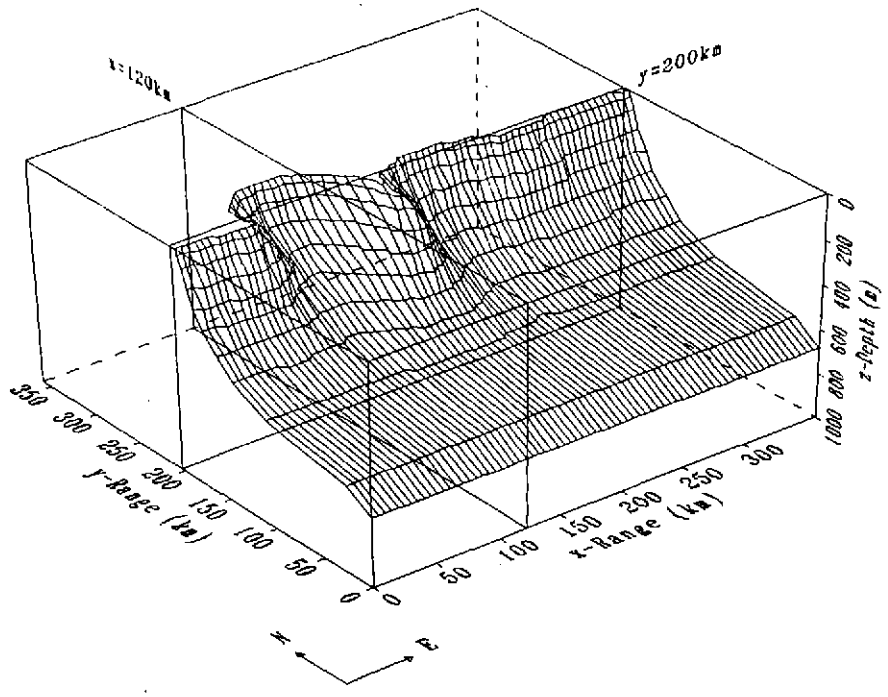

Figure 4. 3-D view of 6 °C isothermal surface 8 days after initialisation with baroclinic perturbation.

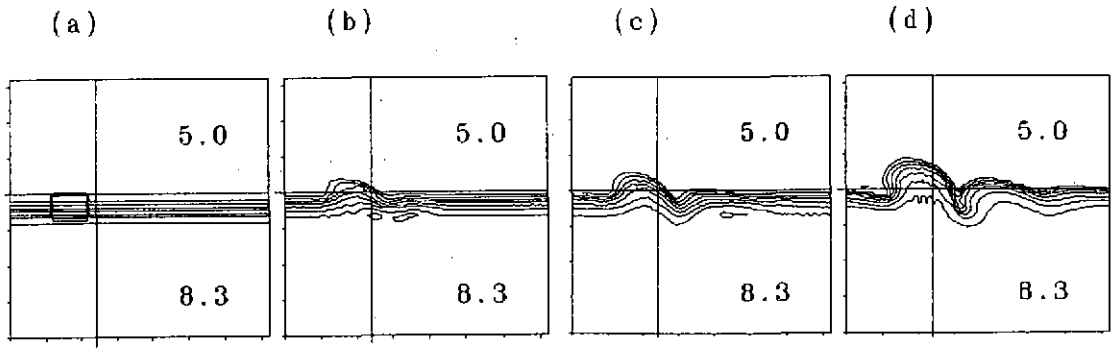

Figure 5. Isotherms at 12.5 m depth (a) 0 days, (b) 2 days, (c) 4 days and (d) 8 days after baroclinic initialisation. Temperatures in the bulk of the water on either side of the front are given. Contour interval 0.5 °C.

COUPLED OCEAN-ACOUSTIC MODELLING

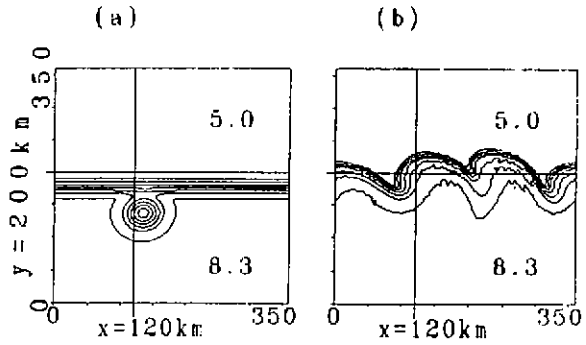

Figure 6. Isotherms at 12.5 m depth (a) 0 days and (b) 16 days after initialisation with a discrete eddy. Temperatures in the bulk of the water on either side of the front are given. Contour interval 0.5 °C.

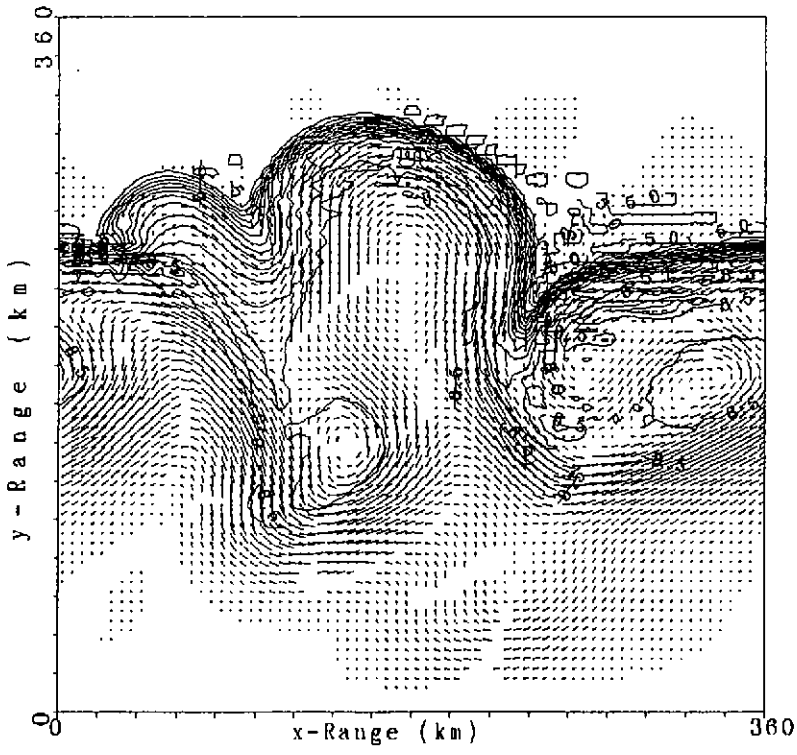

Figure 7. Surface current vectors superimposed on isotherms at 12.5 m depth 24 days after baroclinic initialisation.

COUPLED OCEAN-ACOUSTIC MODELLING

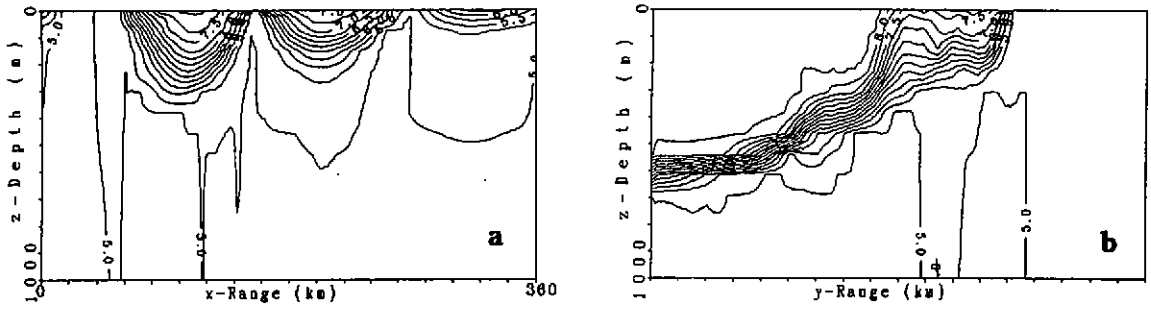

Figure 8. Vertical cross-sections (a) E-W along front (y = 200 km) and (b) N-S through front (x = 120 km), 8 days after baroclinic initialisation (see Figure 4). Contour interval 0.25 °C.

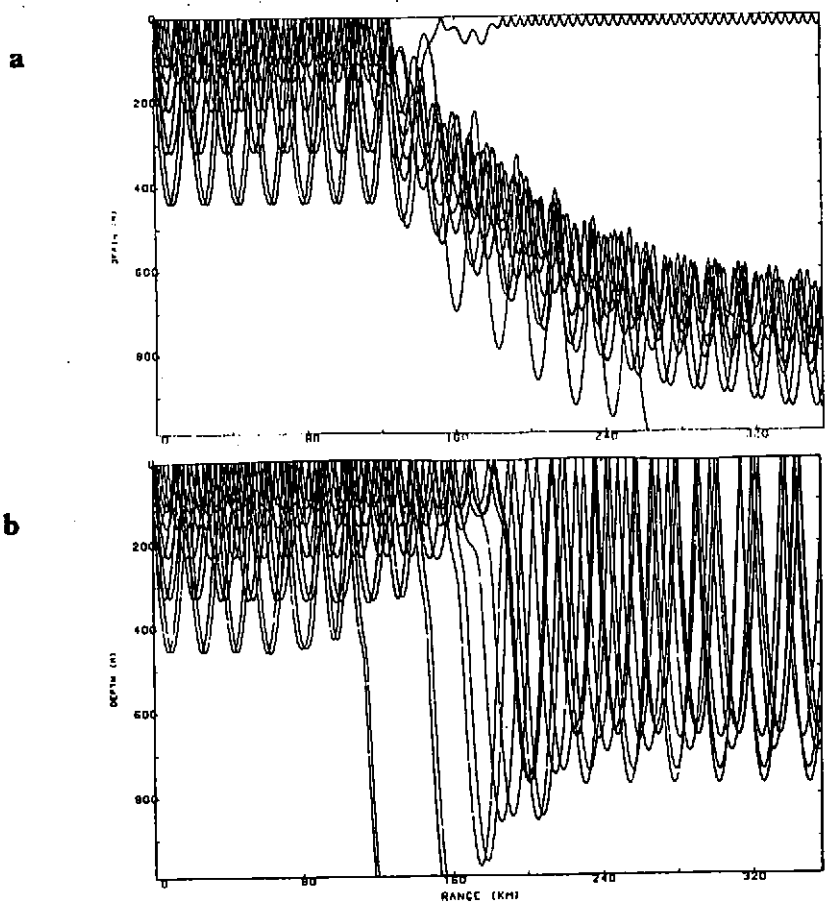

Figure 9. Ray traces (a) S to N and (b) N to S along the x = 120 km cross-section of Figure 8b.

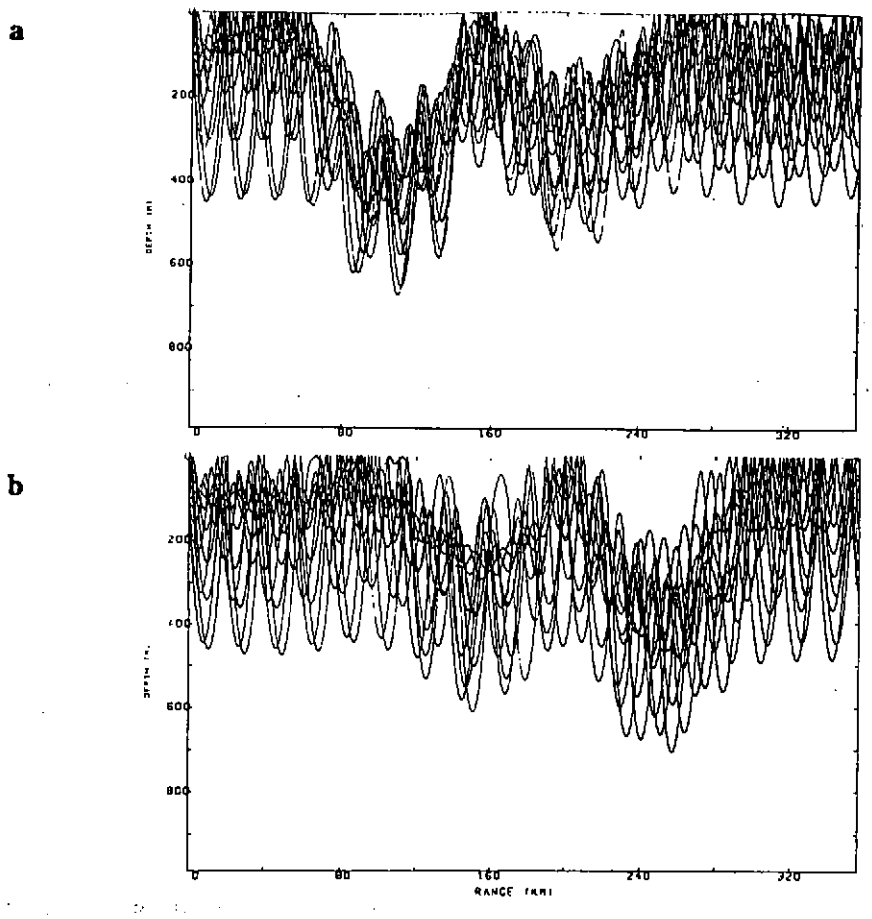

Figure 10. Ray traces (a) W to E and (b) E to W along the y = 200 km cross-section of Figure 8a.

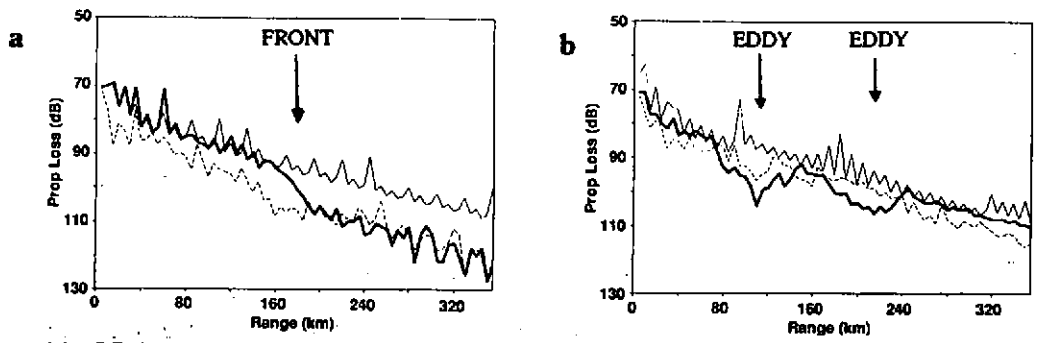

Figure 11. GRASS propagation loss curves for sections (a) through and (b) along front. Results are shown for a frequency of 1 kHz, and for source/receiver depths of 100/100 m (thick line) and 100/250 m (broken line). The range-independent case (thin line) is shown for 100/100 m only.

COUPLED OCEAN-ACOUSTIC MODELLING

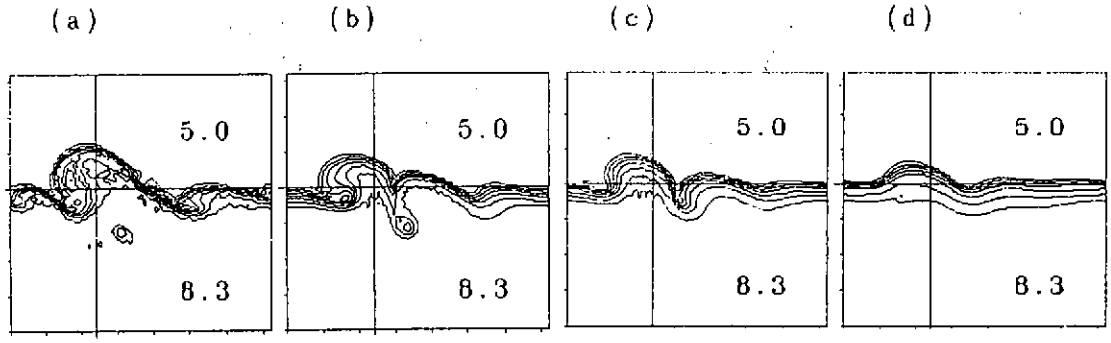

Figure 12. Isotherms at 12.5 m depth at 8 days for horizontal eddy viscosity parameter, A_H, values of 0.1 x 10^7, (b) 0.5 x 10^7, (c) 10^7 and (d) 2 x 10^7 cm^2 s^{-1}.

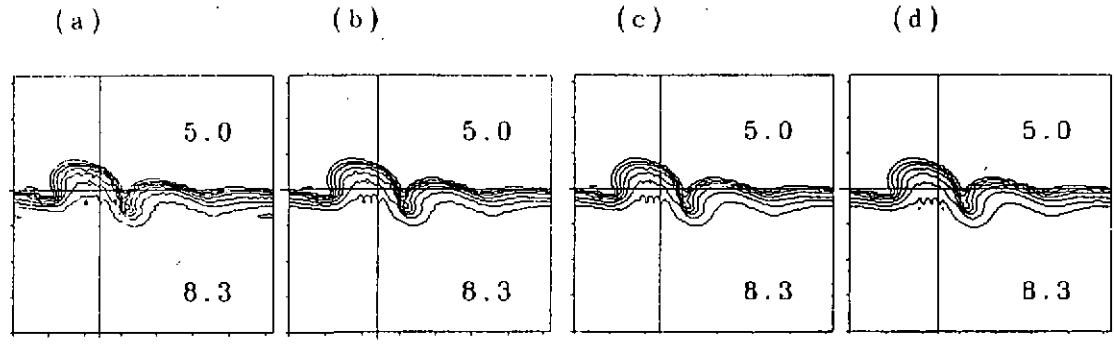

Figure 13. Isotherms at 12.5 m depth at 8 days for horizontal eddy diffusion parameter, K_H, values of 0.1 x 10^5, (b) 0.5 x 10^5, (c) 10^5 and (d) 2 x 10^5 cm^2 s^{-1}.

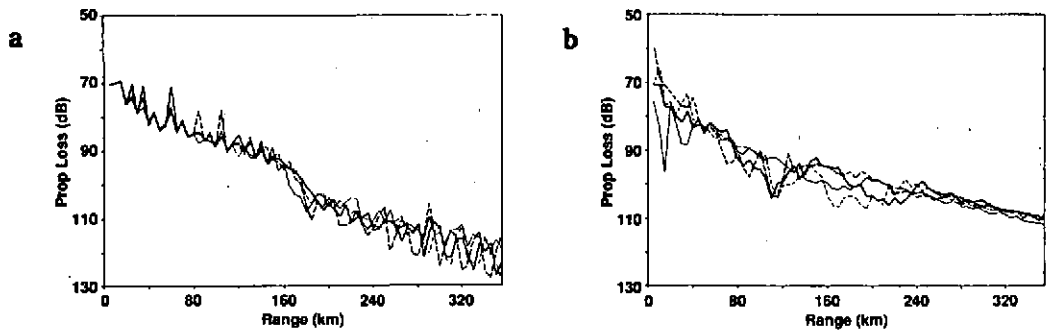

Figure 14. Composite diagrams showing variations in propagation loss on sections (a) through and (b) along front at 8 days for different values of A_H ranging from 0.1 x 10^7 to 2 x 10^7 cm^2 s^{-1} (see Figure 12). GRASS calculations at 1 kHz for source and receiver depths of 100 m.

COUPLED OCEAN-ACOUSTIC MODELLING

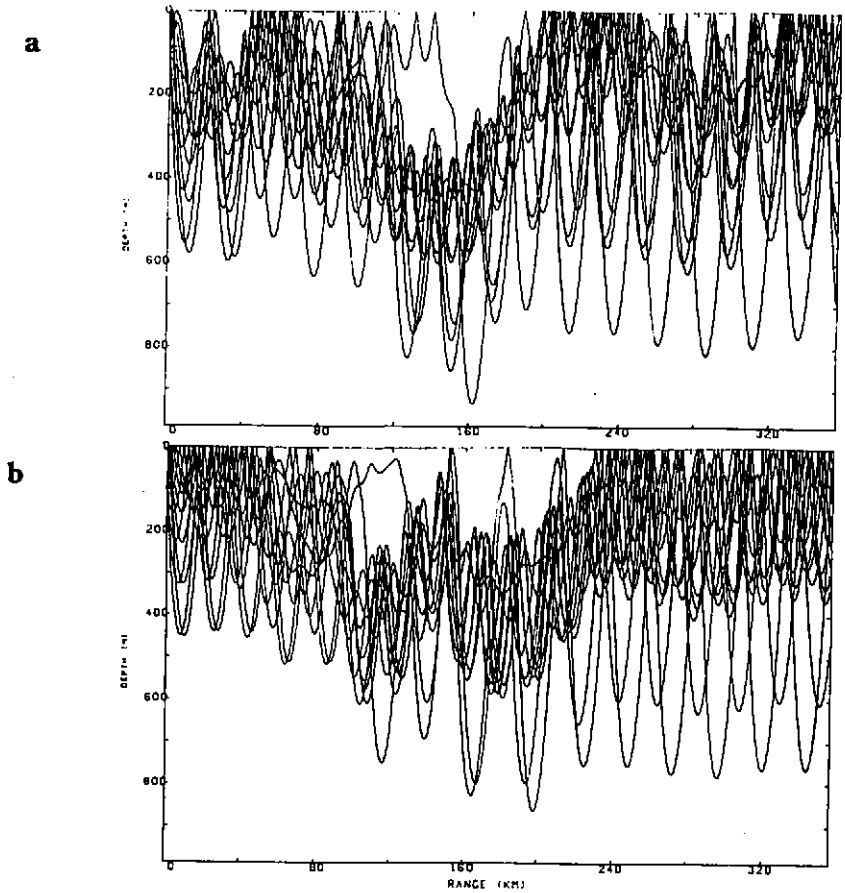

Figure 15. Ray traces along the front (y = 200 km) at 8 days, for A_H values of (a) 0.1 x 10^7 and (b) 0.5 x 10^7 cm^2 s^{-1}.

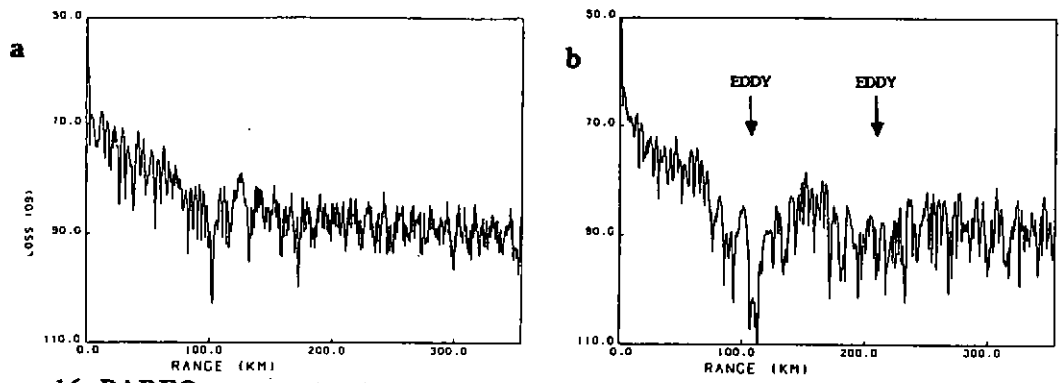

Figure 16. PAREQ propagation loss curves at 150 Hz for sections along the front (y = 200 km) at (a) 2 days and (b) 8 days after baroclinic initialisation. Results are shown for a high bottom loss case, and source and receiver depths of 100 m.